System Design and Optimization of a Hypersonic Launch Vehicle

A project present to
The Faculty of the Department of Aerospace Engineering
San Jose State University

in partial fulfillment of the requirements for the degree
Master of Science in Aerospace Engineering

By

Matthew Ringle

May 2014

approved by

Dr. Papadopoulos
Faculty Advisor

San José State
UNIVERSITY

TABLE OF CONTENTS

LIST OF FIGURES

LIST OF TABLES

1.0 LITERATURE REVIEW

1.1 Background

On October 4th, 1957 a satellite called Sputnik was launched as the first satellite into space. [1] This was the beginning of the greatest decade of aerospace engineering and collaboration of the United States. May 25th, 1961 President John F. Kennedy Spoke to Congress and the nation saying "I believe that this nation should commit itself to achieving the goal, before this decade is out, of landing a man on the Moon and returning him safely to Earth. No single space project in this period will be more impressive to mankind or more important in the long-range exploration of space; and none will be so difficult or expensive to accomplish." [2] This was the beginning of the need for a hypersonic launch vehicle to launch satellites and humans into space, as well as return them safely from space. Since then there has been 16 families of rockets, government and commercial, to launch payloads into orbit. Of those 16 rocket families 5 rockets were used in transporting humans to and from space over the next 5 decades. [3] 2011 was the last time the United States had a vehicle capable of launching humans into space. Over the last 50 years there have been many projects that involved the direct use of long range hypersonic design. The recent cancellation of the third falcon flight funded by DARPA means that there are many questions left to be answered.

Hypersonic velocity is everything that travels above Mach 5. Above Mach 5 it can be expected to endure high aerodynamic heating due to thin shock layers and the dissociation and ionization of air. There are three(3) types of hypersonic vehicles that have been designed; Waveriders, Winged Bodies, and Blunt Reentry Bodies. Comparison of different hypersonic bodies can be seen in Figure 1.
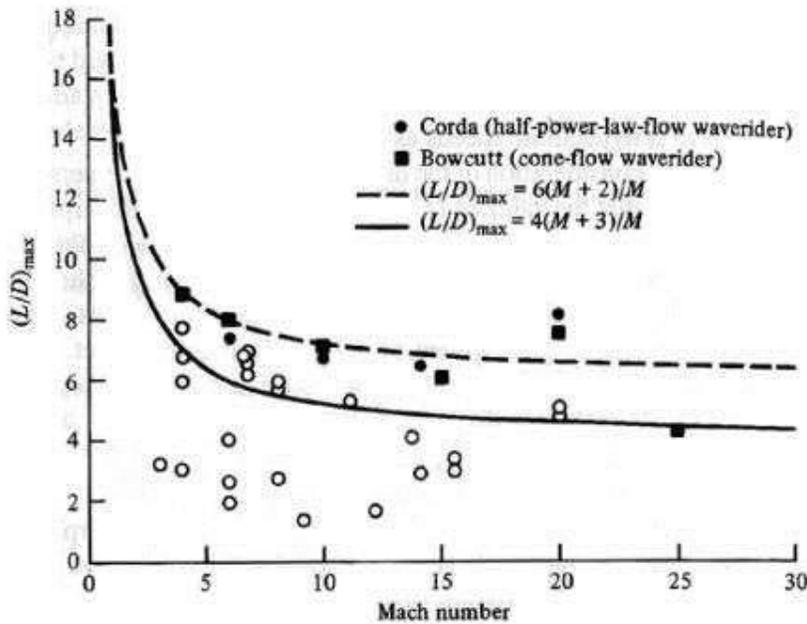
Figure 1: Maximum L/D Ratio Comparison for Various Hypersonic Configurations [4]

Seen in Figure 1 is the comparison of the different tested hypersonic bodies. The white dots are the non-waverider design and can be limited by the Kuchemann equation given by the solid line. This equation is based on data obtained from actual flight data. The solid dots and squares are viscous optimized waverider designs which lie above the Kuchemann line. This means that these designs break the L/D barrier and are more closely characterized by the dashed line.

1.2 Waverider

A waverider is a supersonic aerodynamic configuration with a gasdynamic shockwave attached everywhere along its leading edge at a particular design Mach number and orientation. [5] A depiction of the recently cancelled HTV-2 can be seen in Figure 2.

Figure 2: HTV-2 [6]

The waverider utilizes the shockwave to create a high pressure zone on the windward side of the craft that allows for higher lift. The sharp leading edge allows for the minimization of the spillage from the lower surface to the upper surface. This spillage allows for the high pressure flow to communicate with the lower pressure flow and creates a higher wave drag. This however is an idealized case for the waverider. Due to the sharp leading edges the shock wave is attached and creates a point of high heat transfer along the leading edge. Therefore the leading edge needs to have a radius of curvature in order to detach the shockwave from the edge which in turn results in spillage from the high pressure region to the low pressure region and therefore decreases the performance of the vehicle. This vehicle is advantageous when a mission is requiring a high L/D ratio for longer range at high Mach numbers.

1.3 Winged Bodies

A fixed-wing aircraft is an aircraft capable of flight using wings that generate lift caused by the vehicle's forward airspeed and the shape of the wings. [6] There were two(2) major designs that were tested in the fixed wing category; the Space Shuttle and the X-15. The most known winged hypersonic body is that of the Space Shuttle. It was a fixed wing craft that produced the lift and allowed for the controlled descent from Space at Mach 25. Due to the hypervelocities that was attained by the shuttle it had extremely high heat transfer due to the dissociation of the air around it creating a plasma environment.

Figure 3: X-15 [6]

The X-15 seen in Figure 3 however was flown in the 1960's and is the first manned successful attempt to go hypersonic speeds under powered flight. It reached a maximum Mach number of 6.72. It utilized stubby wings for stability and control. The winged bodies present a problem when achieving hypervelocities. There is high drag associated with wings and stabilizers and the high pressure communicates highly with the low pressure area due to the spillage from the bottom of the body and wings to the top which also decreases the performance of the craft.

1.4 Blunt Reentry Bodies

Reentry Bodies are bodies with low ballistic coefficients on reentry into the atmosphere in order to bring them to subsonic speeds for landing. Reentry bodies have been used since man was first launched into space on the Mercury Program. They utilize a large detached shockwave like the winged bodies in order to dissipate the heat load that occurs on reentry. There are no control mechanisms for use on reentry however so maneuvering is non-existent. They are widely used on launch vehicles still today with the Orion Capsule on the Space Launch System and the Dragon Capsule from SpaceX. Figure 4 shows the Apollo 11 Space Capsule on display at the National Air and Space Museum.

Figure 4: Apollo 11 Capsule. [7]

Depicted in Figure 4 is the Apollo 11 Capsule that reentered the Earth's atmosphere on July 24. It is a blunt body design with an ablative thermal protection system in order to manage the high heat load attained during the reentry phase of the flight.

2.0 PROBLEM STATEMENT

System designs of hypersonic vehicles have been evolving over the past 50 years starting with the X-20 Dynasoar and ending with the recently cancelled Falcon DARPA project. This project and research will focus on the main subsystems of the hypersonic launch vehicle such as the aerodynamics, structures, propulsion, and thermal protection. In order to create a hypersonic launch vehicle there are 2 main tasks that need to be completed; fully couple the system and then optimize the system.

2.1 Fully Coupled System

A coupled system is a set of subsystems designed so that the design of each subsystem relies on the other subsystems. This means that the outputs from one subsystem can be the inputs of another below it or the outputs of one subsystem might be the inputs to another above it as well. This idea of a coupled system is easily depicted with an N^2 diagram.

The N^2 diagram is a depiction of the system broken down into its individual subsystems where the inputs and outputs can be seen as connecting lines to other subsystems. An example of an N^2 diagram can be seen in Figure 5.
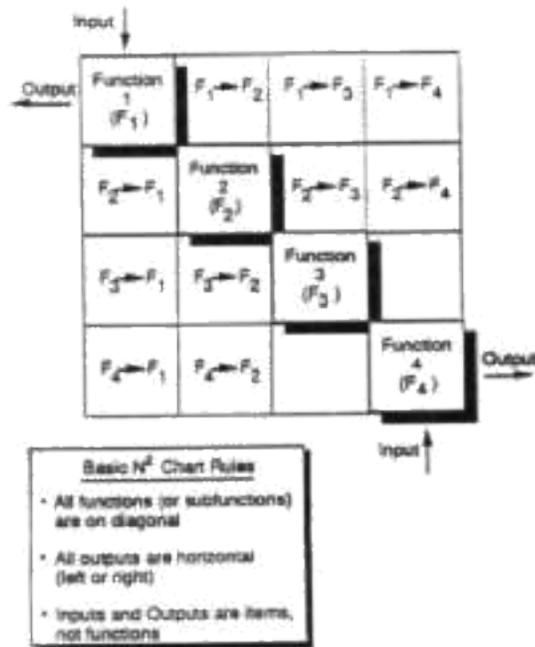
Figure 5: N² Diagram Example [8]

As can be seen in <u>Figure 5</u> is the N² diagram from the NASA Systems Engineering Handbook. This is a very good example as it shows how each output and input relates to a specific function in the diagram.

The individual subsystems of a hypersonic launch vehicle that is being designed in this research are aerodynamics, structures, thermal protection, and propulsion. These subsystems will be placed into an N² diagram and the inputs and outputs will be designed such that the analysis being completed for one subsystem will directly affect either one or more subsystems following, creating a fully coupled system.

2.2 Optimized System

After an initial system is designed from the N² diagram the system can be run through an optimizer. An optimizer is a tool that designs the system to be more efficient given certain merits. These merits can be variables in the system such as lift-to-drag ratio, mass, size, thrust, etc. An optimizer will take the variable that the operator wants to optimize and runs through the N² diagram such that the variable is minimized or maximized with respect to the system. The optimizer is a powerful tool that allows for the coupled design to be analyzed given certain constraints. For this project the merit being optimized the length of the vehicle. By minimizing the length the mass will decrease therefore decreasing the thrust and propellant required.

3.0 DESIGN SPECIFICATION

This hypersonic launch vehicle will be a single-stage-to-orbit, SSTO, design. It is assumed that the waverider will be launched at a velocity of 600 ft/sec from the ground. For payload delivery purposes the altitude needed to be able to have a second stage take the payload into further orbit

9

will need to be at least 250,000 ft. In order for the waverider to have global range it will need to be able to have a a cruise Mach of at least 18. Finally the need for payload delivery is important so the waverider will have a payload capacity of at least 2000 lbs. A sample trajectory can be seen in [Figure 6.](#)
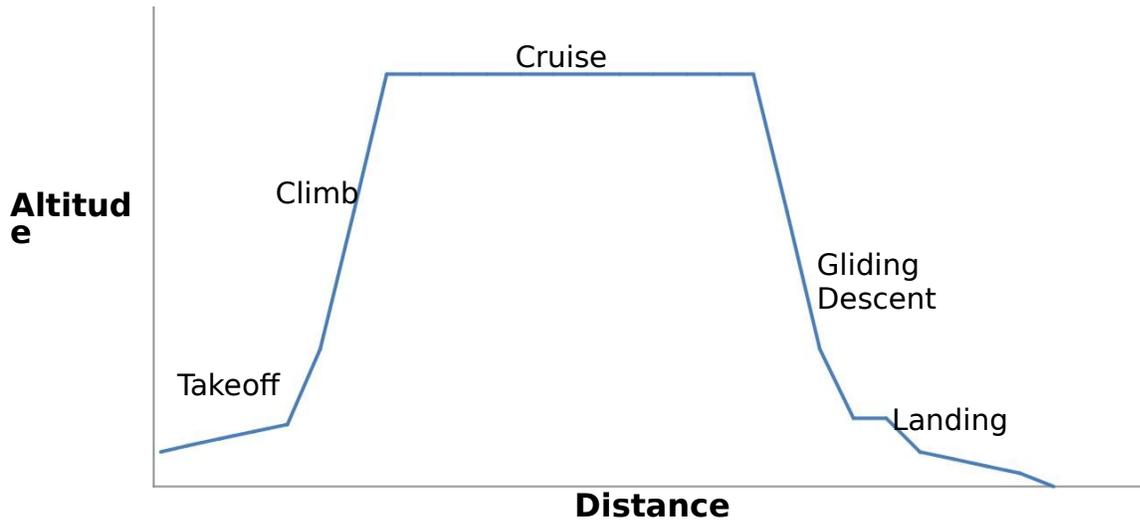
Figure 6: Sample Trajectory

Seen in [Figure 6](#) is a sample trajectory for a mission with respect to an arbitrary maximum altitude and distance. A given trajectory will be used in order to determine the final design.

4.0 SUBSYSTEM PRIMARY GOVERNING EQUATIONS

4.1 OML Subsystem

When designing the OML of the vehicle the shockwave angle, β, is specified and the turning angle, θ, is calculated using the relations for an oblique shockwave. [4]

$$\left[\quad \underline{\qquad\qquad\qquad} \quad \right]$$

Where β is the shockwave angle, γ is the ratio of specific heats, and $\quad$ is the freestream Mach number.

4.2 Rocket Propulsion Subsystem

The propulsion subsystem consists of both the propulsion aspect such as the thrust, time-to-accelerate, and fuel and oxidizer masses and volumes as well as the structural component such as the tanks required for housing the fuel. In the following subsections the propulsion and structural components governing equations will be addressed.

4.2.1 Propulsion Governing Equations

In order to design the propulsion system the thrust needed in order to determine the required burn time. The thrust, F, is calculated using assumed values of time-to-accelerate, t, and change in velocity, v. [9]

$$\overline{}$$

Where W is the dry mass of the system and D is the calculated drag.

The number of engines is required in calculating the volume of fuel and oxidizer needed onboard. The thrust is specified from the previous equation. [9]

$$()$$

Where assumed values of exit velocity, Ve, exit area, Ae, and mass flow rate, for the specific engine is used

The mass and volume of the fuel and oxidizer is important in sizing the craft for the mission. The fuel mass and volume equations are seen below.

$$\overline{}$$

Where is the mass flow rate of the fuel, t is the time-to-accelerate, and is the density of the fuel chosen. The mass and volume of the oxidizer utilizes the same equations as above with the respective changes to the inputs for the oxidizer.

4.2.2 Propulsion-Structural Governing Equations

The volume of the tanks required can be calculated using the volume of either the fuel or oxidizer depending on which tank is being calculated. The need for a frustum tank was evident in order to decrease the length of the vehicle. The two radii and the volume of the fuel tank equations are seen below.

$$\frac{())}{())}$$

$$\overline{}\,(()\ ())$$

Where P_P is the location of the payload bay, P_L is the overall length of the payload bay, and F_L is the length calculated for the fuel tank.

4.3 Thermal Protection Subsystem

Thermal protection is separated into three categories the conduction, convection, and radiation. Conduction is the calculated using Fourier's Law. [10]

Where is the change in temperature from the outer surface to the inner surface, k is the thermal conductivity constant and A is the surface area.

The convection is calculated using the 1-D convection equation. After specifying the convection coefficient, h, the surface area, A, and the change in temperature, ΔT from the flow to the surface the power can be calculated. [10]

The heat transfer related to radiation can be calculated by using the Stephan-Boltzmann Law. [10]

Where ε is the emissivity, A is the surface area, σ is the Stephan-Boltzmann constant, and T is the temperature. All three equations are used when determining the heat transfer through the thermal protection system.

5.0 SUBSYSTEM DESIGN

Parameterization is important when designing a concept so that when analyzing, the design can be changed with a few variables. The outer-mode-line (OML) and the structural designs are both parameterized with respect to the beta angle, Mach number and the overall length of the vehicle. Including the three other subsystems will have their own parameterizations and when integrated will have an effect on the entire system as well.

5.1 Parameterized Waverider Design

A design of a hypersonic vehicle's OML requires an inverse design method. An inverse design method utilizes the flow field given certain parameters and designs the vehicle such that certain aspects of the vehicle are optimized. The most common flow field used for utilizing the inverse design method is the wedge flow field.

In order to utilize the wedge flow field for the design of the waverider a two-dimensional wedge

is used. This wedge requires the Theta-Beta-Mach tables for the flow field design. Given a certain beta angle and Mach number the theta, flow turning, angle can be calculated using oblique shock theory. The basic design can be seen in Figure 7.
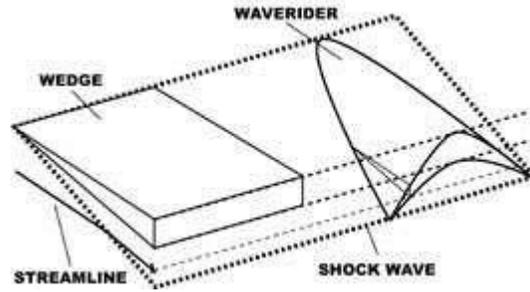
Figure 7: Wedge-Derived Waverider [11]

Depicted in Figure 7 is the basic design of the wedge-derived waverider. This will be used in determining the final design of the vehicle. Because the design is based on the Mach number and beta angle means that the design can be changed for the different inputs.

The generating flowfield and subsequently the waverider design can be seen in Figure 8.
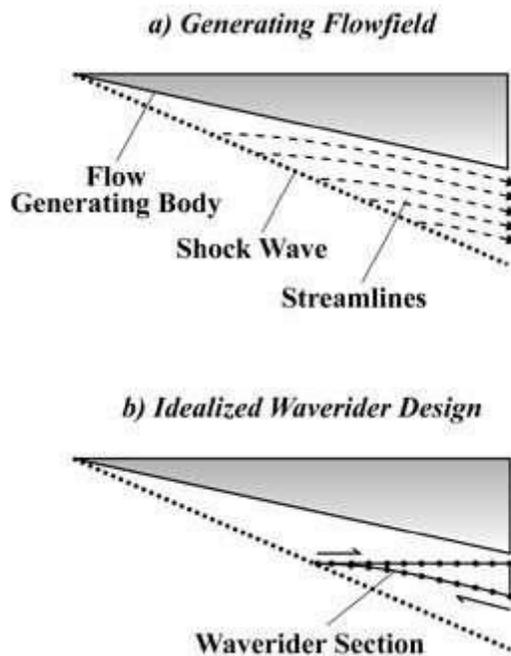
Figure 8: Waverider Creation from a Generating Flowfield [11]

As shown in Figure 8 is the generalized generating flowfield. This flowfield depicts the body, produced shockwave, beta angle, and the turning streamlines, theta angle, with respect to the windward body. The waverider is therefore designed such that the lower sharp edges are the same angle as the shockwave and the turning flow is the interior of the vehicle. This will provide maximum pressure on the windward side of the waverider. Sharp edges are used due to the minor leakage from the lower flow to the upper flow. In actuality this will produce high heating and a

13

radius of curvature will need to be added to allow for manufacturing and heat load.

A slice of the parameterized waverider design can be seen in Figure 9.

Figure 9: Wedge Body Slice

It can be seen in Figure 9 that the upper surface of the waverider is parallel to the freestream velocity while the lower surface is equal to the turning angle that is calculated with respect to the chosen flowfield conditions and the position of the slice.

The process of taking slices of the vehicle is repeated until the model in Figure 10 is seen below.
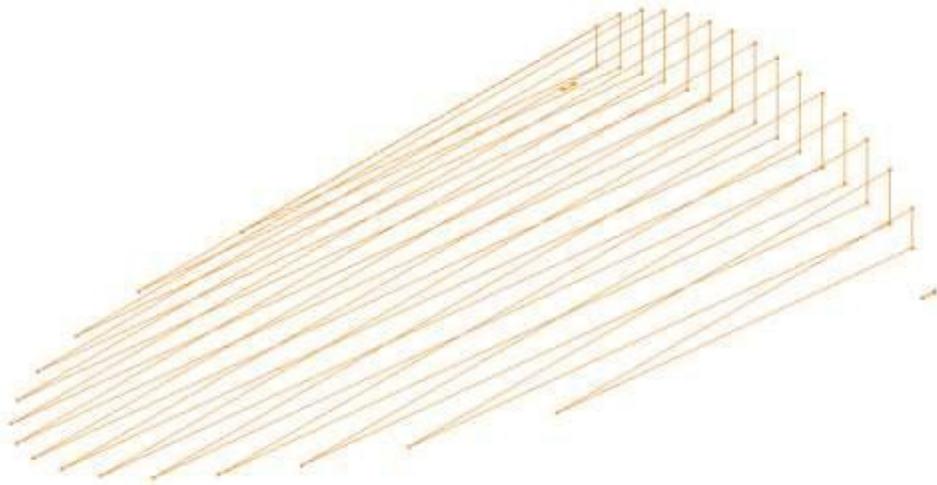
Figure 10: Full Model Slices

Figure 10 shows the model as slices that were designed with respect to the flowfield conditions. The slices not only provide the upper and lower surfaces of the vehicle but also the leading edge of the craft. This is completed by the lower surface having a curvature using an equation of an ellipse. The point of the wedge is then placed on the chosen shockwave angle such that the leading edge is riding on the shockwave. This minimizes the spillage from the lower high pressure region to the upper low pressure region.

The initial solid parameterized waverider design can be seen in Figure 11.
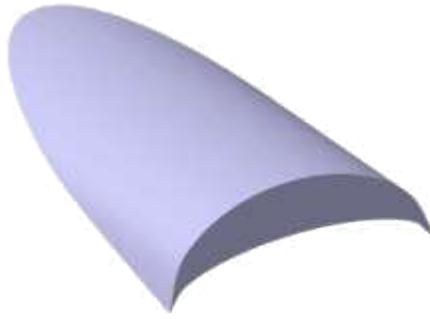
Figure 11: Parameterized Waverider Outer Mode Line Design

Seen in Figure 11 is the parameterized waverider design. This design is parameterized with respect to the beta angle, Mach number and the length of the vehicle. The curvature of the lower surface is calculated using the equation of an ellipse. This should funnel the flow towards the center of the lower surface increasing lift. Having the OML parameterized upon three variables will allow for quick changes to the design of the craft upon analysis.

For the present work completed the flowfield properties are predominately 2-dimensional. Due to the nature of the flowfield means that using exact theory has potential to have a higher accuracy. Given the chosen shock angle from the generated flowfield the properties after the flow can be calculated using the exact theory equations:

$$\_\_\_ \quad \frac{\left(\_\_\_\right)}{\overline{\underline{}}} \frac{\left[\_\_\_\right]}{}$$

$$\_\_ \quad \_\_\_$$

The flow properties that were calculated from a Mach number of 18, shock angle of 10° and standard temperature and pressure at 250,000 ft after the oblique shockwave can be seen in Table 1.

Table 1: Exact Theory Calculations

Flow Properties	Calculated	Units
Mach 2	6.01	
Pressure 2	19.03	Pa
Density 2	1.15E-04	Kg/m^3
Temperature 2	303.25	K

Seen in Table 1 are the calculations that were completed for the flow properties after the oblique shockwave. It is seen that the pressure and temperature after the shockwave is 19.03 Pa and 303.25 K respectively and the Mach number is 6.01.

5.2 Parameterized Propulsion Design

Hypersonic propulsion is achieved either with air breathing technology such as scramjets or rocket technology. Due to the mission requirements the only possible propulsion is the rocket propulsion because of the high Mach number of 18. Therefore the equations for rocket propulsion are utilized.

The propulsion system is designed in a Matlab code authored by myself in order to size the fuel required, fuel mass, tank sizing, and tank mass. The inputs to the program can be seen in Table 2. These inputs are for the NK-33 rocket engine.

Table 2: Propulsion Engine Inputs

Engine Input Variable	Inputs [12]
Chamber Pressure (psf)	302839.12
Chamber Temperature (R)	6618.6
Isp (s)	331
(lb/sec)	825
(lb/sec)	319
Exit Pressure	~0
Exit Area	33.798
Throat Area	1.252
γ	1.24
(lb/ft^3)	63.67
(lb/ft^3)	50.31
Weight	621704
Tank Material Density	169.86

As seen in Table 2 are the inputs to the propulsion system design program. The program calculates the thrust required as well as calculate the volume of fuel and oxidizer required. The structural masses of the two tanks required are also calculated.

The propulsion system program has been benchmarked against the first stage of the Antares/Taurus II rocket. The analysis can be seen in Table 3.

Table 3: Antares/Taurus II Propulsion Benchmark

	Antares/Taurus II 1st Stage	Calculated	Percent Error
Fuel Mass (lb)	142727	151692.76	6.28
Oxidizer Mass (lb)	390791	392308.87	0.39
Burn Time (s)	235	237.76	1.18
Total Length of Tanks (ft)	90.55	83.1	8.23
Thrust (lbf)	734000	732846.4	0.16

As seen in Table 3 is the benchmarked data compared to the calculated data. It can be seen that the percent error is maximum on the total length of the tanks and the lowest is on the thrust of the system. The 8% error is most likely due to the material choice of aluminum for the tanks as well as the fact that the connections and thermal protection were not calculated. It is shown that the program is within an acceptable 10% of the benchmark data.

5.3 Parameterized Structural Design

Roskam gives good initial design rules for the structural layout of the fuselage of commercial airplanes, fighters, and large transports. The fighter due to its supersonic flight velocity is the chosen design consideration that will be utilized initially. Roskam gives frame depths, spacing and longeron spacing guidelines for each layout. [13] The fighter layout usually has a frame depth of about 2 inches, a frame spacing of 15-20 inches and a longeron spacing of 8-12 inches. A diagram of the definition of the longeron spacing, frame depth and frame spacing can be seen in Figure 12.

Figure 12: Frame Depth, Frame Spacing, Longeron Spacing Diagram

As seen in Figure 12 are the guidelines of the frame depth, frame spacing and longeron spacing. It is shown that the frame depth is the cross-sectional height of the frame, the frame spacing is on center from one from to the next and the longeron spacing is the spacing between the supports that run the length of the fuselage.

The completed construction lines of the waverider given the previously discussed guidelines can be seen in Figure 13.
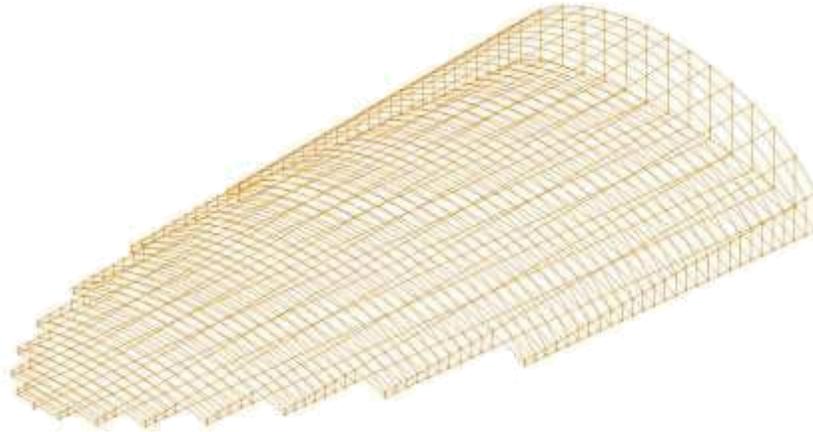
Figure 13: Waverider Construction Lines Isometric View.

As shown in Figure 13 are the construction lines for the structural subsystem of the waverider given the guidelines used from Roskam. The spacing of the frames is on average about 15 inches and the longeron spacing is 31.25 inches. This spacing is higher than the guideline due to the fact that stiffeners will be added to increase the strength of the OML.

The top view of the waverider allows for the ease of seeing the spacing of the construction lines. This spacing can be seen in Figure 14.
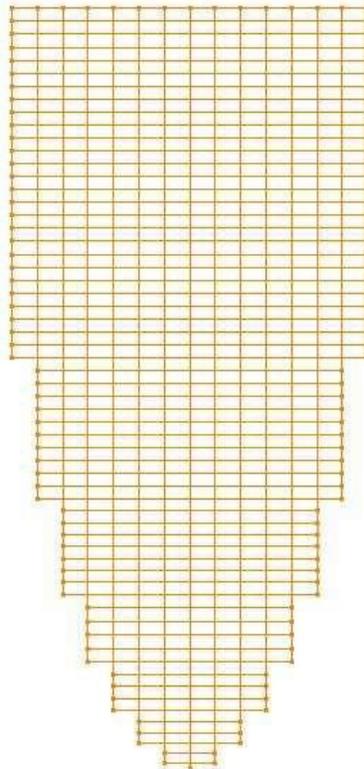
Figure 14: Waverider Construction Lines Top View.

As depicted in Figure 14 the construction lines show that the frame spacing is on average 15 inches and the longeron spacing is about 31.25 inches. With the addition of stiffeners between the

longerons the spacing will be decreased to the guidelines by Roskam [13].

The initial structural parameterized design can be seen in Figure 15.
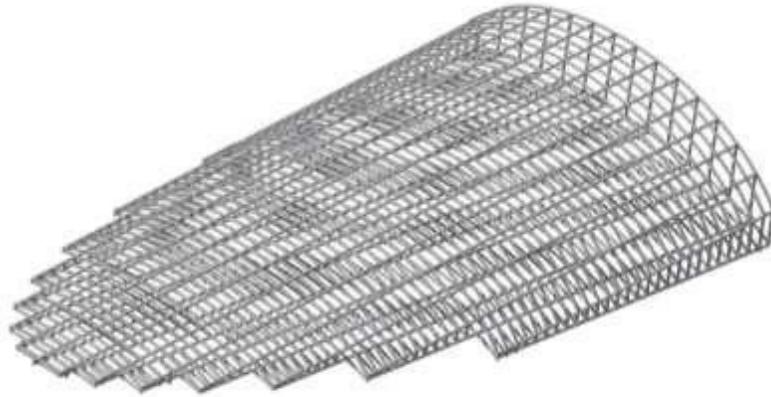
Figure 15: Parameterized Waverider Structure Design

Depicted in Figure 15 is the initial structural design for the waverider. The frame cross-section is that of a commercial T-beam with height of 2.575 inches, a width of 5 inches, a flange thickness of 0.43 inches, and a web thickness of 0.27 inches.

The rear view of the structure can be seen in Figure 16 below.

Figure 16: Parameterized Waverider Design Rear View.

Depicted in Figure 16 is the rear view of the vehicle. This view shows that the windward side of the vehicle is not straight but curved using the equation of an ellipse. This curvature should allow for the funneling of the high pressure air to the center of the vehicle creating more lift while decreasing the spillage loss from the lower to the upper surface. Also seen in the view is the spacing between the longeron. This spacing will allow for the more stiffeners to be attached directly to the substructure which will add rigidity while keeping the mass of the vehicle lower.

An initial analysis was completed on the structure the structure had the rear of the vehicle constrained and an acceleration due to gravity placed down as is the craft were flying level. A material of Aluminum-Lithium (AA 2090) was selected due to its low density of 0.0936 lb/in^3 but high strength of 75400 psi for initial analysis. From the hand calculations the pressure after the shockwave was placed upward to determine the total deformation as well as where the Von-Mises

19

stress occurs. The total deformation analysis can be seen in Figure 17 and the Von-Mises stress can be seen in Figure 18.
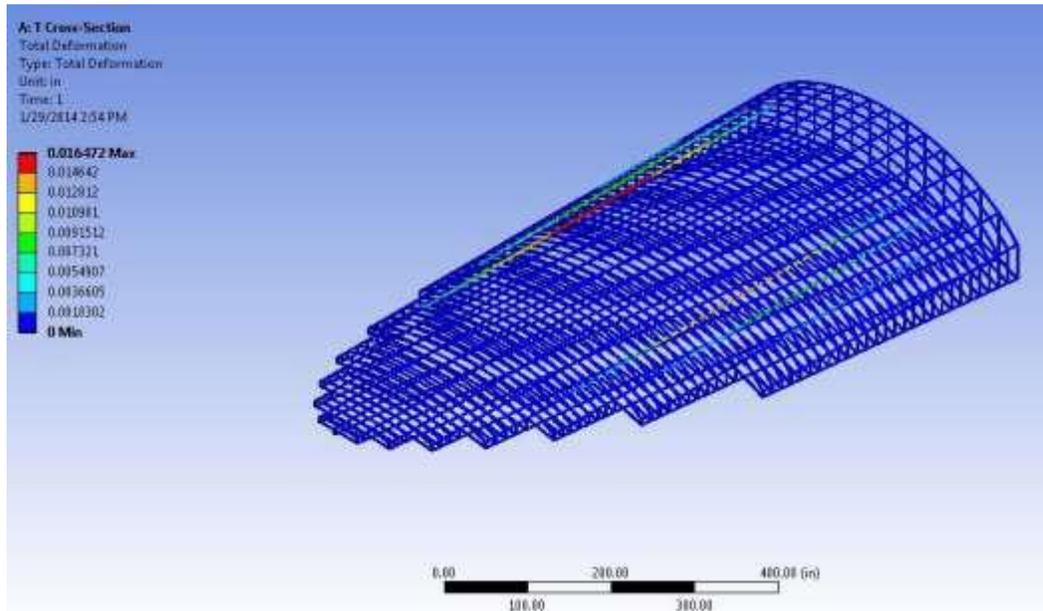
Figure 17: Total Deformation Structural Analysis From Hand Calculated Pressure.
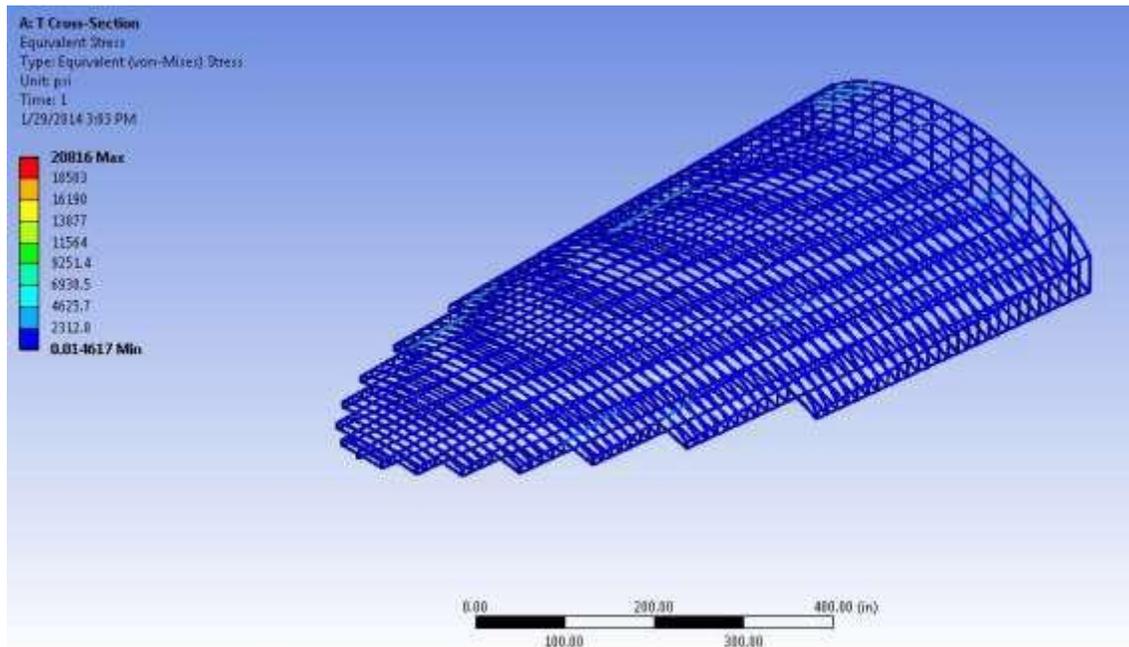
Figure 18: Von-Mises Stress Structural Analysis From Hand Calculated Pressure

As can be seen in Figure 17 the maximum deformation that occurs on the structure is 0.0165 inches. Such a small deformation without any of the supports required is negligible. This means that possibly some of the frames might be taken out of the structure upon further analysis. In Figure 18 the stress is seen to be 20816 psi it is also seen that the maximum stress occurs on the top of the vehicle where gravity will affect the long level beams more. Calculating the factor of

safety by dividing the maximum stress that occurred on the structure by the yield strength of the material will yield a factor of safety of 3.62. As an initial analysis this is acceptable as a factor of safety.

6.0 SYSTEM INTEGRATION

As discussed earlier the N^2 diagram is the most important aspect for the design on a hypersonic vehicle. The N^2 diagram is a depiction of how the subsystems interact with one another and can be rearranged so that the process is optimized. Figure 19 depicts the N^2 diagram for the hypersonic waverider that was designed for this project.

					Payload Length Payload Radius		Payload Length
Payload Length	Payload Length				Payload Position		Payload Position
	Trajectory	Mach Dynamic Pressure Angle of Attack			Mach, Time to Acceleration		
		Geometry Outer Mode Line			Turn Angle		
		Aerodynamics	Temperature Convection	Pressure	Drag		
			Thermal			Thermal Mass	
				Structures		Structure Mass	
				Thrust	**Propulsion**	Propulsion Mass	Fuel Tank Length Oxidizer Tank Length
	Total Length				Dry Mass	**Mass**	**Total Length**

Figure 19: Hypersonic Waverider N^2 Diagram.

As seen in Figure 19 is the N^2 diagram for the hypersonic waverider that is being analyzed for this project. The placement of the major subsystems was such that the coupling of the subsystems was minimized. It can be seen that the only coupling that exists are between the Propulsion and Mass subsystems and the Total Length and Geometry Subsystems.

The N^2 diagram starts with the payload length subsystem. This subsystem takes the Space Shuttle knowledge of the volume of payload bay required for a certain amount of mass to be carried to low Earth orbit. This subsystem then scales the volume required for the mass of the payload for the waverider to lift. The radius of the payload bay is then chosen and a length is determined. The data is then exported into the Geometry subsystem, Propulsion subsystem, and Total Length subsystem. The second block is the trajectory subsystem. This subsystem takes an existing trajectory that has been flown and exports the data into the Aerodynamics subsystem and Propulsion subsystem. The third block is the Geometry subsystem. This system imports the payload length and an assumed initial total length and changes the total length of the waverider. The program then exports the OML design into the Aerodynamics subsystem and the turn angle into the Propulsion subsystem. The fourth block is the Aerodynamics subsystem which imports

the surface triangulated OML as well as the Mach, dynamic pressure, and Angle of Attack from the Trajectory block and completes the Aerothermal analysis for the trajectory chosen. This data is then exported into the Thermal, Structures, and Propulsion subsystems. The fifth block is the Thermal block which imports the temperature and convective heat transfer data from the Aerodynamics subsystem. The analysis is completed to determine that the heat transfer through the chosen thermal protection system is adequate and the TPS mass is exported into the Mass Subsystem. The sixth block is the Structures subsystem which imports the pressure data from the Aerodynamics subsystem and completes a structural analysis on the basic structure to determine the deformation that occurs on the maximum pressure during the trajectory. The structure mass is exported into the Mass subsystem. The Propulsion subsystem is the seventh block on the N^2 diagram. This subsystem imports data from the Payload Length, Trajectory, Geometry, and Aerodynamics subsystems and determines the mass and volume of the fuel and oxidizer required, the mass and length of the fuel and oxidizer tanks, and the thrust and number of engines required for the given ascent trajectory. The propulsion mass and tank lengths are then exported into the Mass and Total Length subsystems. The eighth block is Mass subsystem where it imports the various masses from the Thermal, Structures and Propulsion subsystems and the exports the dry mass back into the Propulsion subsystem and this iterates until convergence is met. The last block is the Total Length subsystem. This imports the lengths of the tanks, the payload position and payload length and determines the total length required for the system. This length is then exported into the geometry where the N^2 diagram is run through again until the length is optimized for the given parameters.

7.0 OML TRADE STUDIES

Two trade studies were completed in order to determine the optimal Beta angle to be used when generating the geometry. The position of the payload was initially analyzed as can be seen in Table 4 as well as the L/D was determined for a range of Angle of Attacks seen in Table 5. These trade studies determined the optimum beta angle to be 10°.

Table 4: Payload Position vs. Beta Angle

Mach	Beta (°)	Turn Angle (rad)	Payload Position (ft)
18	5	0.043090473	139.16
18	10	0.130134146	30.56
18	15	0.206908319	28.58
18	20	0.280509059	20.83

Table 5: Beta Angle vs. L/D

Case	-20	-15	-10	-5	0	5	10	15	Percent Difference
Waverider-5	-2.66	-3.54	-5.04	-7.48	4.23	6.06	4.17	3.05	0
Waverider-10	-2.66	-3.5	-4.85	-3.78	5.82	4.15	2.94	2.28	3.96
Waverider-15	-2.64	-3.43	-4.28	2.68	4.21	3.14	2.42	1.94	24.26
Waverider-20	-2.61	-3.31	-1.48	3.51	3.23	2.51	1.99	1.62	42.08

As seen in Table 4 is a trade study that was completed in order to determine where the payload

would be located in the waverider given the radius required. It was found that the when the beta angle was increased the payload position was decreased. The payload position ranges from 6.3 ft. from the nose up to 139 ft. The first choice would be to have a larger beta angle therefore decreasing the total length of the waverider. A second study was needed in order to determine how the L/D would change with respect to the beta angle. This study can be seen in Table 5. A test of various geometries with different beta angles was conducted at various angles of attack and the L/D was calculated in order to determine the best beta angle to use for the analysis. It can be seen that the maximum L/D of 6.06 was achieved at a beta angle of 5° and the L/D decreased with increasing beta angle. L/D needs to be maximized for the longest range; therefore the 5° beta angle would be optimal. Given both trade studies the choice of a beta angle of 10° was chosen due to its low percent difference from the maximum L/D at 3.96% and a payload position of 30.56 ft. from the nose.

8.0 SYSTEM OPTIMIZATION

In order to determine the optimal length for the system Phoenix Integration's Model Center was used in order to connect the inputs and outputs from each subsystem in the N^2 diagram. First an initial guess was conducted. This guess resulted in a craft that would be able to complete the mission with a fuel tank length of 42.17 ft. and an oxidizer tank length of 39.03 ft. Seen in Table 6 also are the radii for the various tanks. It was determined early on that conducting the analysis with a single cylindrical tank the length grew exponentially. The decision was then made to create frustum tanks. These are tanks that are conical in shape with a smaller beginning radii and larger end radii. This allowed for the tanks to decrease in length and create a craft that was manageable in size. Due to the need for the length to be optimized and therefore reducing the mass of the vehicle, the system was iterated upon itself until the total calculated length of the system reached within 1 ft. of the input length. These iterations can be seen in Table 6 below.

Table 6: System Length Optimization

Iterations	Initial Guess (ft)	Fuel Radius 1 (ft)	Fuel Radius 2 (ft)	Fuel Length (ft)	Ox Radius 1 (ft)	Ox Radius 2 (ft)	Ox Length (ft)	Total Length (ft)
1	150	3.98	6.74	42.17	6.74	9.29	39.03	141.99
2	140	3.98	6.52	38.85	6.52	8.94	37.01	136.65
3	130	3.98	6.32	35.79	6.32	8.61	35.09	131.66
4	131.66	3.98	6.41	37.10	6.41	8.76	35.92	133.81
5	135	3.98	6.48	38.26	6.48	8.88	36.65	135.69
6	135.69	3.98	6.42	37.32	6.42	8.78	36.06	134.16

As shown in Table 6 as the six iterations that were needed for the total length to converge on a minimum given the initial inputs. Each iteration took into account the position of the payload bay, the payload bay length, fuel tank length, and the oxidizer tank length. Since the payload bay position and length are set by initial conditions and the beta angle the tanks are the lengths that are changing with respect to the total mass of the design. From the initial design length of 150 ft. the total calculated length of 141.99 ft. was determined. In order to determine the lower limit of the convergence a second initial guess of 140 ft. was chosen which resulted in a total calculated

length of 136.65 ft. A third initial guess of 130 ft. was the lower limit of the convergence which resulted in a total length of 131.66 ft. It was then iterated using the calculated lengths until a convergence was met within 1 ft. at 135 ft. as seen in iteration 5 and was verified with iteration 6.

9.0 RESULTS AND DISCUSSION

9.1 Waverider Final Design

After the optimization of the length of the vehicle the final design OML of the waverider can be seen in the following figures.
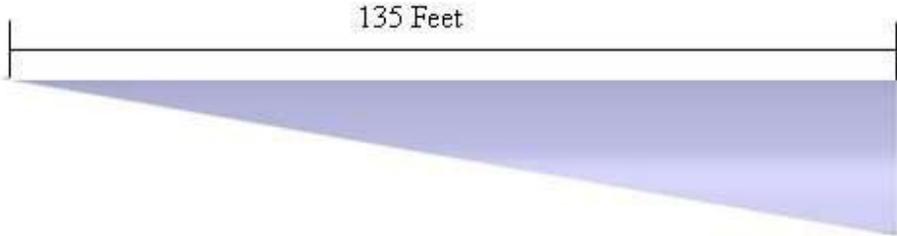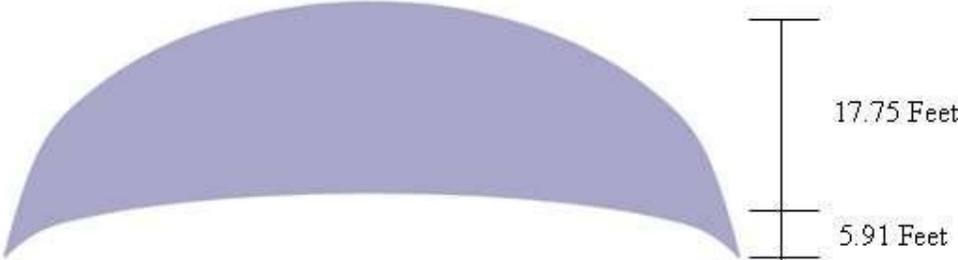

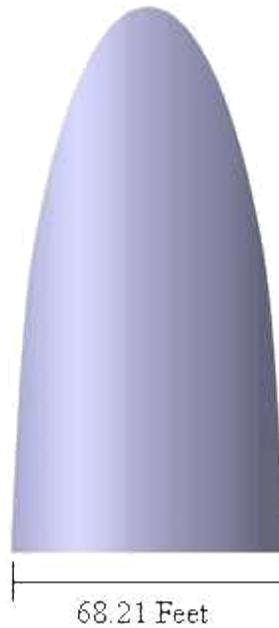**Figure 20: OML Final Design Left View**

Figure 21: OML Final Design Rear View

Figure 22: OML Final Design Top View

Depicted in Figure 20, Figure 21, and Figure 22 are the final designs of the OML after the optimization. It is seen that the total length is 135 ft., the height of the usable space is 17.75 ft., the total height is 23.66 ft., and the span of the vehicle is 68.21 ft.

The inputs into CBAERO for the Aerothermal analysis can be seen in Table 7 below

Table 7: CBAERO Inputs

CBAERO Inputs	Value
Centroid x (m)	28.992
Centroid y (m)	0
Centroid z (m)	-2.416
Reference Area (m^2)	666.15
Chord (m)	41.148
Span (m)	20.789

The inputs to CBAREO that can be seen in Table 7 are the centroid of the OML design, the Reference Area, the Chord and the Span of the vehicle. The values were determined in the CAD model of the OML.

The output values from Phoenix Integrations Model Center can be seen in Table 8

Table 8: Final Design Output Values

Design	Value
Mach	18
Beta (°)	10
Turn Angle (rad)	0.130
Payload Position (ft)	30.564
Payload Length (ft)	30.220
Fuel Radius 1 (ft)	3.978
Fuel Radius 2 (ft)	6.42
Fuel Length (ft)	37.32
Ox Radius 1 (ft)	6.42
Ox Radius 2 (ft)	8.78
Ox Length (ft)	36.06
Length (ft)	134.16

As seen in Table 8 are the output values obtained from the analysis in Model Center. Given the Mach, Beta, and Turning angles it is seen that the initial fuel radius is 3.978 ft., the final fuel radius is 6.42 ft., and the fuel tank length is 37.32 ft.; the oxidizer tanks radii are 6.42 ft. and 8.78 ft. respectively with a total length of 36.06 ft. Given the payload position and payload length the total length would calculate to 134.16 ft. This would be within 1 ft. of the 135 ft. guess.

9.2 Aerodynamics

The aerodynamics subsystem imports the given trajectory into the Configuration Based Aerodynamics (CBAERO) code. For supersonic and hypersonic Mach numbers CBAERO uses a modified Newtonian method for predicting inviscid pressure distributions along each triangle. The entropy is calculated after the normal shock and combined with the surface pressure and an assumption of the process being isentropic the thermodynamic state of the triangle is then calculated. [14]

The given trajectory characteristics can be seen in Figure 23 and Figure 24. Figure 23 is ascent trajectory characteristics used for analysis and Figure 24 is the given descent trajectory characteristics. Both ascent and descent trajectories were used in determining the aerodynamics of the waverider.
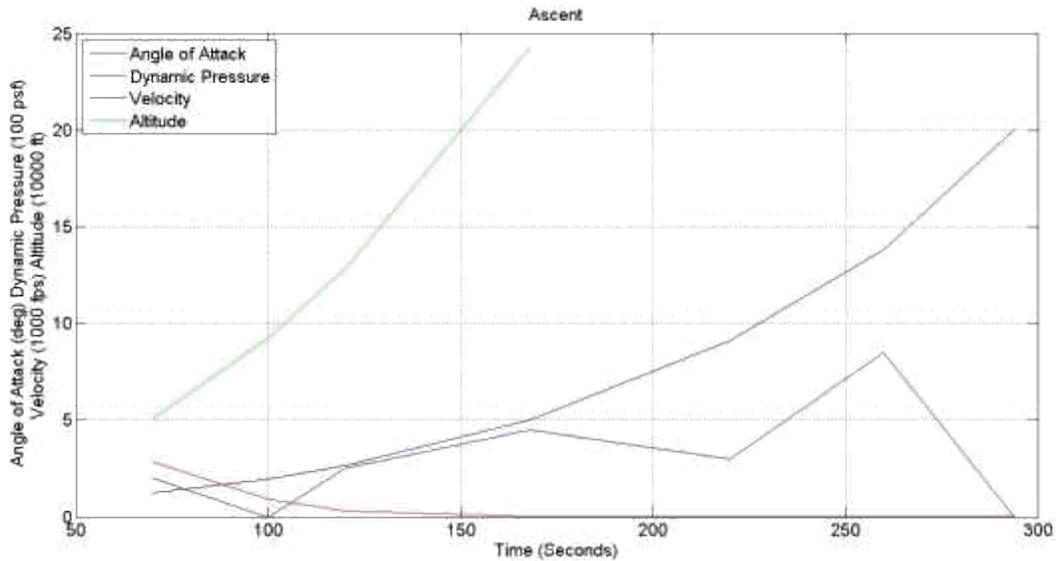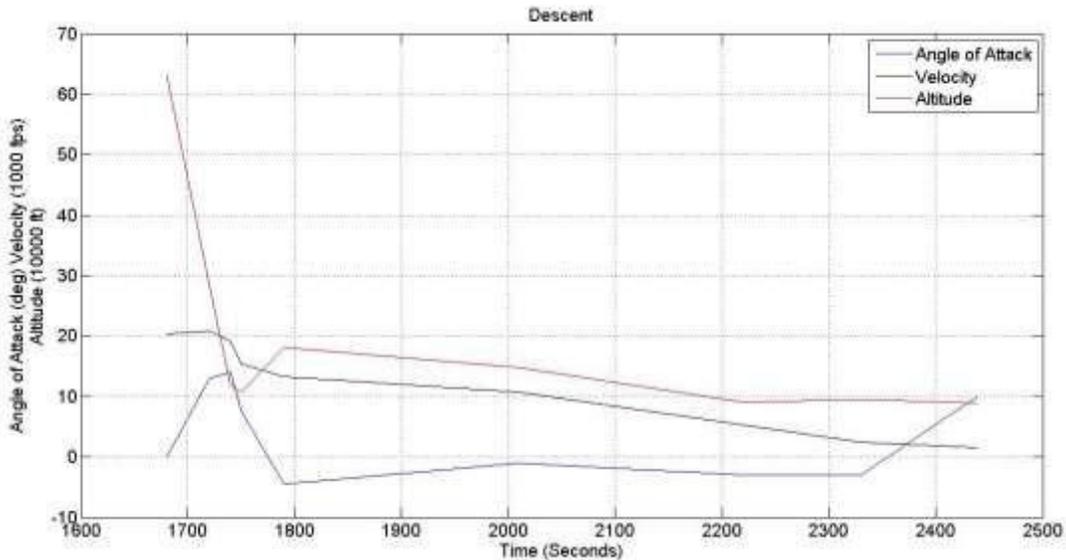
Figure 23: Ascent Trajectory Characteristic

Figure 24: Descent Trajectory Characteristic

As depicted in Figure 23 are the ascent trajectory characteristics that were used in the CBAERO software. As seen the angle of attack changes from 0 to 8 degrees, the dynamic pressure goes from sea level to space, the velocity ranges from 600 fps to 20000 fps, and the altitude ranges from 50000 ft. to about 250000 ft. Seen in Figure 24 are the descent/entry trajectory characteristics that were utilized. The angle of attack ranges from -5 to 14 degrees, the velocity ranges from 20000 fps to about 1500 fps, and the altitude ranges from 600000 ft to about 10000 ft. These characteristics are imported into CBAERO and the various aerodynamics are calculated for the waverider. The streamlines from CBAERO can be seen in Figure 25.
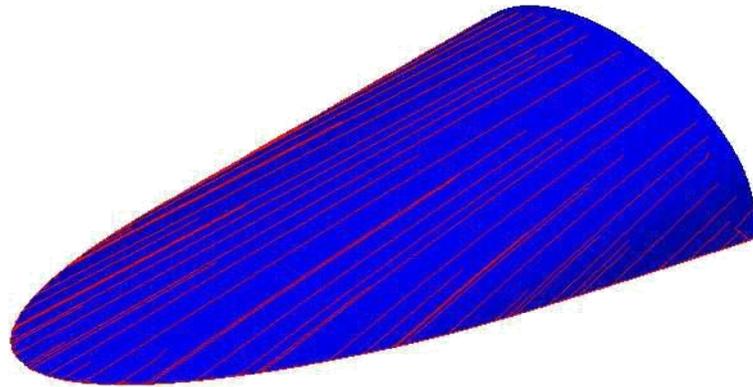
Figure 25: Waverider Streamlines

The streamlines that can be seen in Figure 25 are correct to the body they seem to be coming from the leading edge up to the center of the craft. This is significant due to the fact that it shows that the flow is being funneled to the center of the vehicle creating a high pressure region on the windward side of the vehicle.

The data reduction occurred in a MATLAB code that was designed to take in the raw data from CBAERO and extract the useful data relating to the trajectory that was flown. Figure 26 and Figure 27 depict the L/D vs. Angle of attack for ascent and descent Mach numbers.
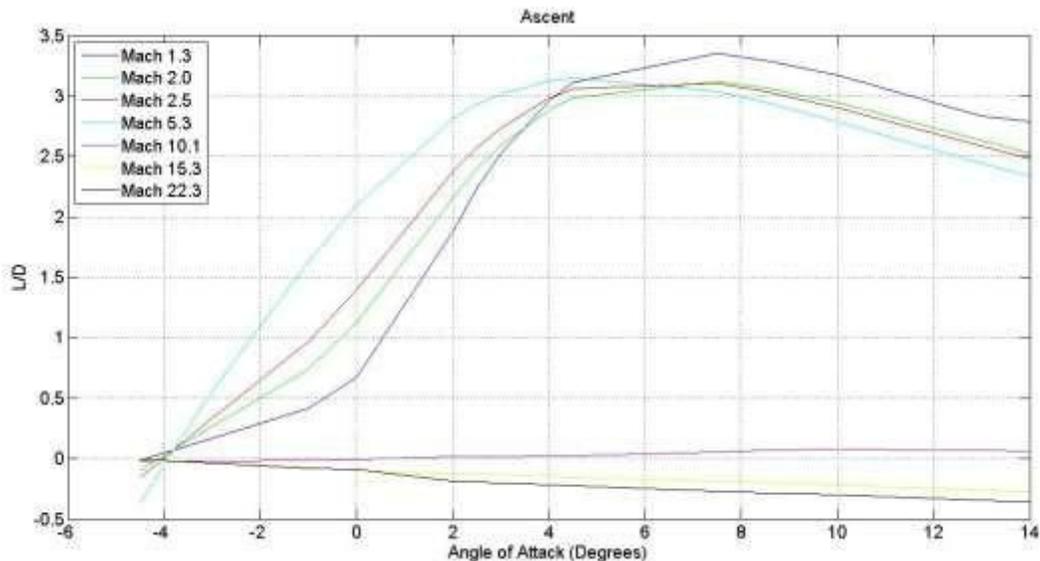
Figure 26: Ascent L/D vs. Angle of Attack

Seen in Figure 26 is the L/D vs. the Angle of Attack. This data is with respect to the specific trajectory point of Mach and dynamic pressure across the range of angle of attack from -5° to 14°. From this graph it is seen that a maximum L/D of about 3.4 is reached at a Mach of 1.3 and a minimum L/D of -0.4 at a Mach of 22.3. The reason for the negative L/D is due to the altitude that the vehicle is at the time. It can also be seen that in Figure 26 the maximum L/D for each Mach

28

changes with the angle of attack. This is a coupling effect due to the dynamic pressure. As the pressure changes the maximum L/D changes as well.

Figure 27: Descent L/D vs. Angle of Attack
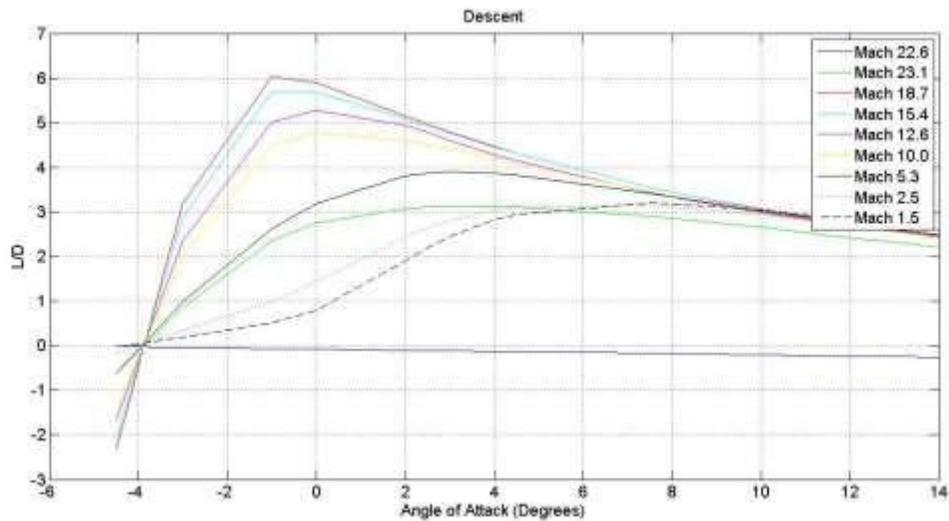
The Descent L/D over the range of angle of attack is seen in Figure 27. This L/D data is with respect to the descent from a maximum Mach of 23.1 to a Mach of 1.51. As seen at Mach 22.6 the L/D is again negative due to the fact that the dynamic pressure is so low there is not enough to create more positive lift. The maximum L/D of 6.0 occurs at the design Mach of 18. This is due to the shockwave being close to the design point and minimizing the spillage over from the high pressure region to the low pressure region. The higher L/D at Mach 18 is expected from the theory of waverider designs.

A history plot for the L/D with respect to time is useful in determining how the waverider behaves during the given trajectory. It can be seen that the L/D is at a maximum of around 4.5 at 2000 seconds and a minimum of -1.5 at about 1750 seconds. This history plot can be seen below in Figure 28.
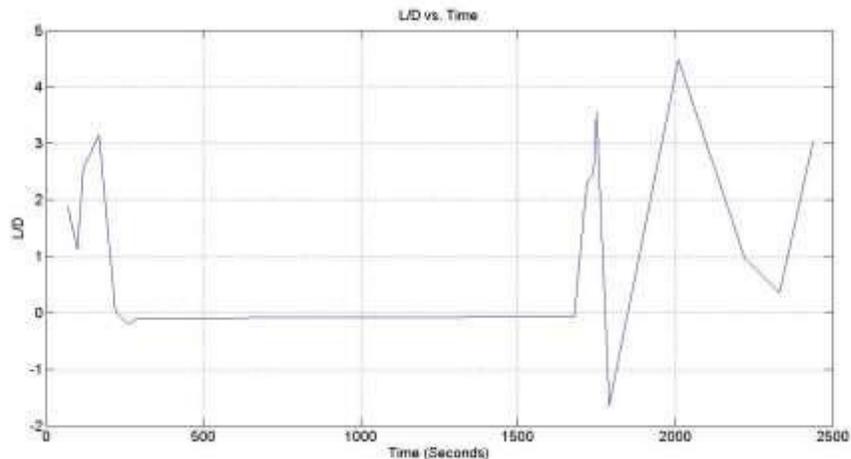

Figure 28: L/D vs. Mission Time

A depiction of the pressure, at Mach 18 and an angle of attack of 14°, on the windward side of the vehicle from CBAERO can be seen in Figure 29.
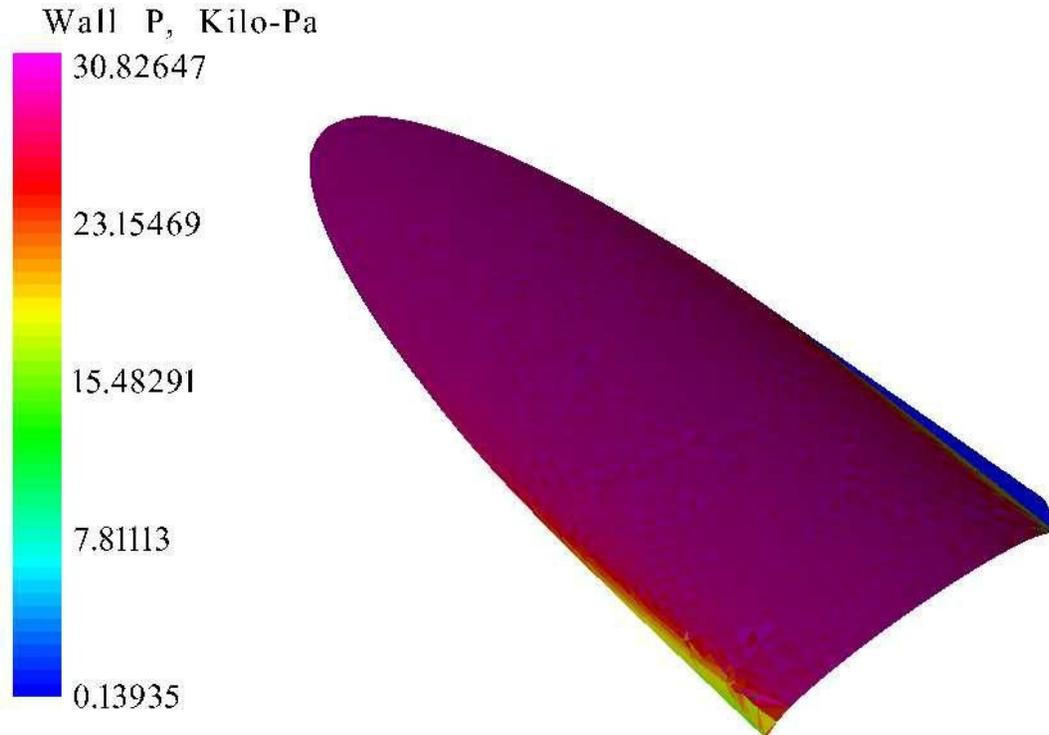

Figure 29: Windward Pressure Visualization

Seen in Figure 29 is the pressure on the windward side of the waverider. This pressure is the maximum pressure that occurs on the vehicle at an altitude of 120000 ft. It can be seen that the pressure is maximum on the center of the vehicle and decreases as it gets to the edge of the vehicle. This is easily seen towards the rear of the vehicle when it goes from the high pink pressure to the lower yellow pressure. This is very important because it proves that the pressure is being funneled to the center of the windward side of the vehicle minimizing the spillage over to the low pressure area.

9.3 Propulsion

The propulsion subsystem was designed in a MATLAB code. This MATLAB code takes the drag from the aerodynamics subsystem and computes the mass and volume of the fuel and oxidizer required, the mass and length of the fuel and oxidizer tanks, the thrust and number of engines required for the given ascent trajectory. The rocket engine that was chosen for the mission was the NK-33 or AJ-26 from Aerojet. This engine has a very high thrust to weight ratio and uses a more dense fuel than the Space Shuttle Main Engine making the volume for the fuel required less. The engine inputs to the MATLAB code is seen in Table 9.

Table 9: MATLAB Propulsion Inputs

Input Variables	Inputs [12]
Chamber Pressure (psf)	302839.12
Chamber Temperature (R)	6618.6
Isp (s)	331
(lb/sec)	825
(lb/sec)	319
Exit Pressure	~0
Exit Area	33.798
Throat Area	1.252
γ	1.24
(lb/ft^3)	63.67
(lb/ft^3)	50.31
Weight	621704
Tank Material Density	169.86
Initial Velocity (ft/sec)	600
Δt (sec)	511
Payload Position (ft)	30.56
Payload Length (ft)	30.22
Drag (lbf)	229292

Seen in Table 9 are the inputs to the MATLAB program that was designed to size the fuel, oxidizer, thrust and number of engines required for the mission. The code requires constants from the engine as well as initial conditions for the mission and the dry mass of the vehicle. The engine inputs that are needed are the chamber pressure, chamber temperature, Isp, oxidizer and fuel flow rate, exit pressure, exit area, throat area, gamma of the chamber and the density of the fuel and oxidizer. The Tank material density is used to determine the total mass of the tanks, the initial velocity, drag, and change in time is used to determine the thrust. The payload position and length sizes the initial radii of the fuel tank followed by the oxidizer tank. The outputs of the program can be seen in Table 10.

Table 10: Propulsion Design Output

Propulsion Design Output	Design
Mass Fuel Tank (lb)	8013.11
Mass Oxidizer Tank (lb)	24127.6
Mass Fuel Required (lb)	169038
Mass Oxidizer Required (lb)	437167
Volume Fuel (ft^3)	3359.93
Volume Oxidizer (ft^3)	6866.14
Fuel Tank Initial Radius (ft)	3.98
Fuel Tank Final Radius (ft)	6.42
Oxidizer Tank Initial Radius (ft)	6.42
Oxidizer Tank Final Radius (ft)	8.78
Fuel Tank Length (ft)	37.32
Oxidizer Tank Length (ft)	36.06
Thrust (lbf)	379975
Number of Engines	1.04

Table 10 portrays the outputs that the MATLAB code provides. The fuel mass, tank mass and volume can be found to be 169038 lb, 8013 lb and 3359 ft^3 respectively and the oxidizer mass, tank mass and volume are calculated to be 437167 lb, 24127 lb and 6866 ft^3 respectively. The radii for the fuel tank 3.98 ft. and 6.42 ft. and the radii for the oxidizer tank are 6.42 ft. and 8.78 ft. Utilizing the frustum style tank allowed for a semi-conformal tank which will decrease the overall length of the tanks. The fuel and oxidizer tank lengths are 37.32 ft. and 36.06 ft. respectively. The trust was calculated to be 379975 lbf required which equates to a number of engines of 1.04. This number of engines can be used with just one engine due to the fact that the thrust can have a power level over 100% but the analysis assumed 2 engines. The two engines can have a decreased power level which will increase the life of the engines and provide reusability over the life of the engine.

9.4 Structural

The structural subsystem was designed in a CAD program that utilizes solid beams with common cross sections. The cross section that was chosen for this design was that of a T. This T cross section design will allow for the thermal protection system to easily attach to the structure. The T cross section is the same as it was in the preliminary design process. The isometric view of the structure can be seen in Figure 30
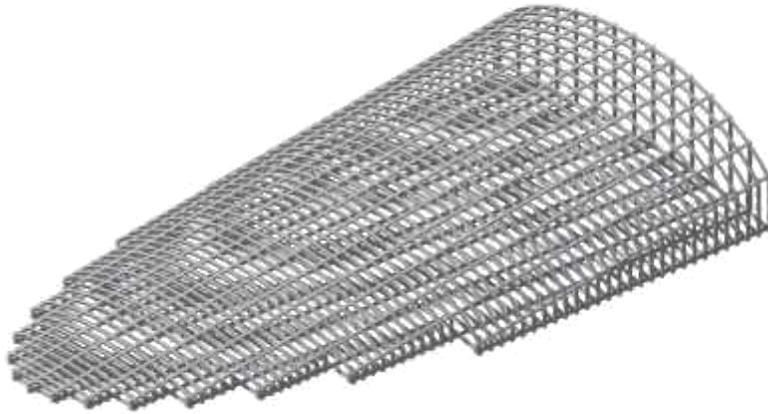
Figure 30: Structure Isometric View

As depicted in Figure 30 the structure is designed with 15 longerons that run the length of the vehicle and numerous stringers that will distribute the load. The structure is designed so that the leading edge of the waverider will be attached away from the primary structure so that the heat transfer from the thermal protection system to the structure is minimized reducing the thermal stresses on the vehicle. The top view of the structure can be seen in Figure 31.
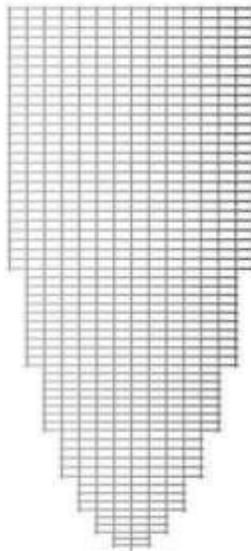

Figure 31: Structure Top View

Seen in Figure 31 is the top view with the stringers and longeron spacing more visible. The average spacing between stringers is 2.35 ft. and the spacing between longerons is 4.34 ft.

9.5 Thermal

The thermal subsystem analysis utilized the thermal data obtained from the CBAERO analysis of the given trajectory. From the data the main heat transfer mechanism was through convection. This convection data for the given time was an input into the analysis program in order to determine if the Thermal Protection System, TPS, was a viable choice. The TPS analyzed was a modified version of a metallic TPS which can be seen below in Figure 32.

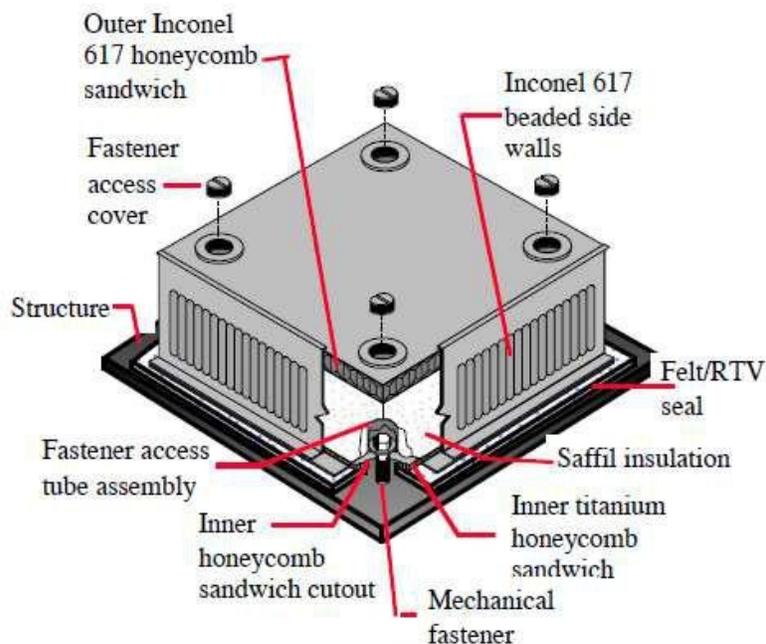**Figure 32: Metallic TPS.**

As depicted in Figure 32 is the metallic TPS system that is being modified for the waverider analysis. The TPS is made up of Inconel 617 honeycomb sandwich panels with a Saffil insulation second and a base aluminum structure layer. Due to the high convection and heating that is occurring on the nose and body of the waverider the Inconel 617 material would not be able survive reentry conditions. Due to this problem the modified design utilizes Reinforced Carbon-Carbon, RCC, Honeycomb sandwich panels as a substitute which would be able to handle the high heating that occurs on the waverider. The second layer of Saffil remains due to the great thermal properties as an insulator and having a high melting point of over 2000 °C. The convection data from CBAERO can be seen in Figure 33 and Figure 34.
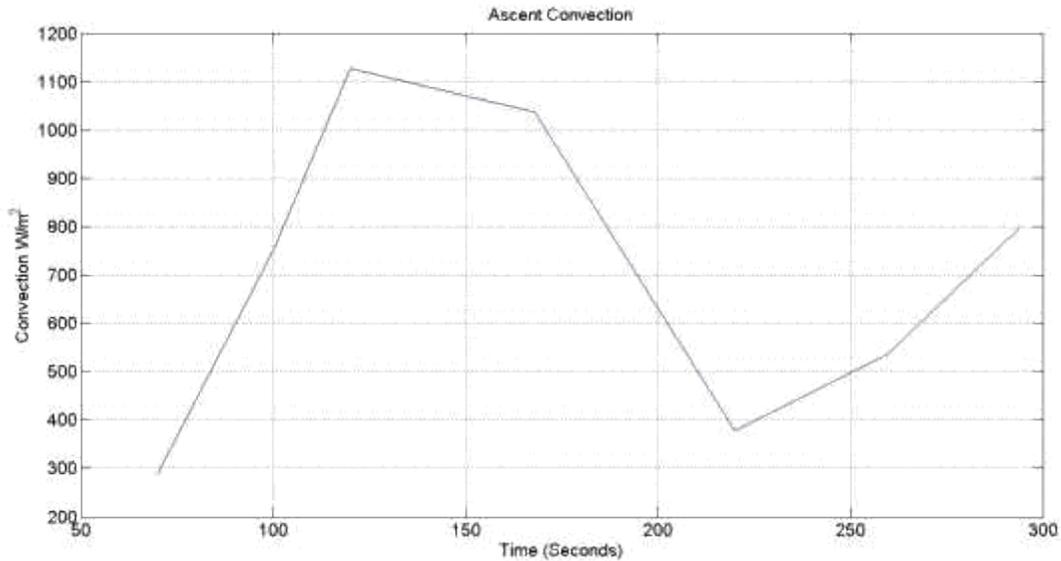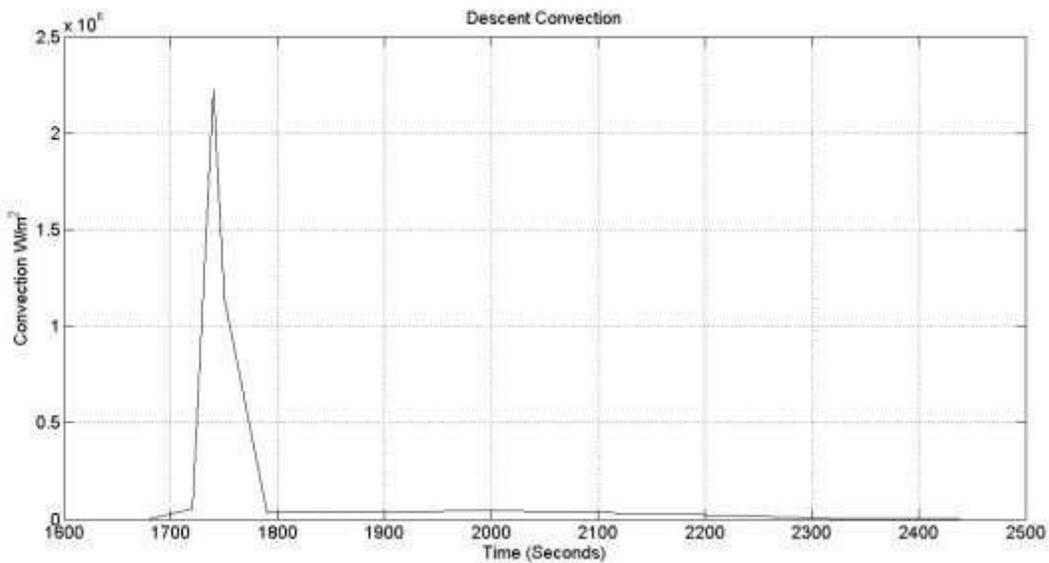
Figure 33: Ascent Convection vs. Time

Figure 34: Descent Convection vs. Time

Seen in the images above are the convection data for the ascent and descent portions of the trajectory. As can be seen the ascent convection compared to the descent convection is much less. The maximum convection occurs at around 1740 seconds into the flight with a value of 2.25 MW/m^2. This is a short duration but drastically increases the heating that occurs over the body. The primary sizing of the TPS is done through the heat load over the trajectory. This is the integrated area under the curve over the trajectory portions. For the ascent trajectory the heat load is 163098 J/m^2, and for the descent trajectory the heat load is 73491375 J/m^2. Due to the high nature of the heat load upon descent, the heat transfer through the TPS will be analyzed to determine if the Aluminum substructure will survive the reentry of the waverider. The thermal analysis setup that was conducted can be seen in Figure 35 below.
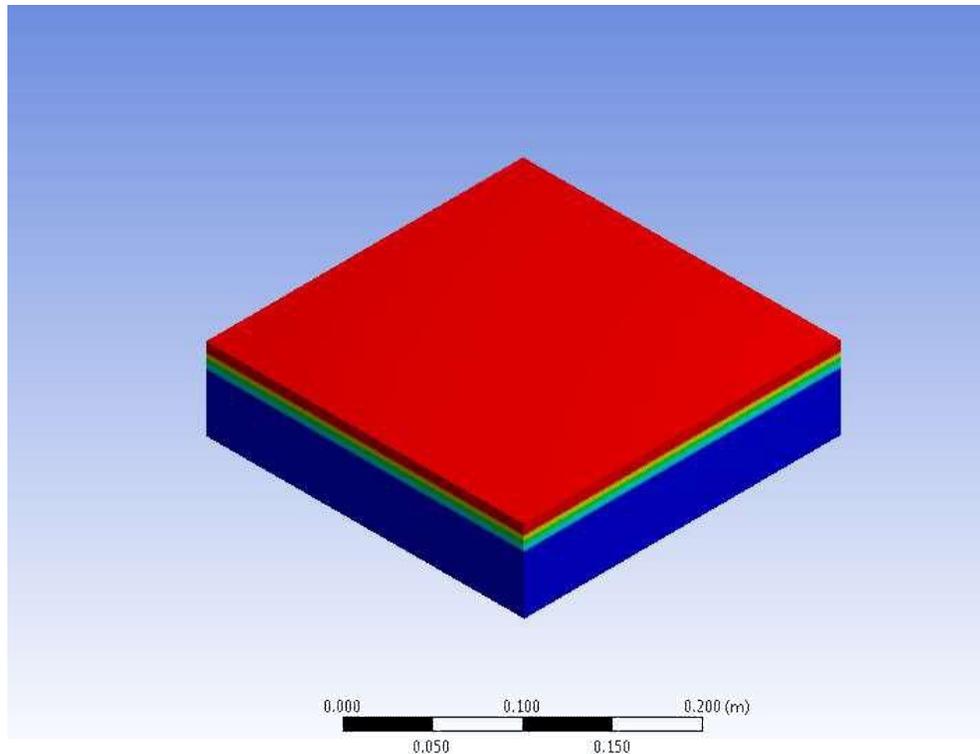
35

Figure 35: Thermal Analysis Setup

As depicted in Figure 35 is the setup for the TPS analysis. Due to the complexity of the system and only the need for the analysis through the material a 0.2 m by 0.2 m section of the windward side of the waverider was taken. The TPS materials are stacked upon each other and assumed to be touching. The RCC honeycomb sandwich has a thickness of 0.0071 m, the Saffil has a thickness of 0.051 m and the aluminum substructure has a thickness of 0.006 m. The material properties for each material can be found in the Appendix. The analysis was completed through the descent trajectory and the atmospheric temperature at the given altitude was used for ambient temperature, as well as a radiation factor between the RCC and atmosphere was placed as a constraint and a radiation factor from the Saffil and the RCC was taken into account. The convection boundary condition was placed on the top RCC honeycomb sandwich which is the outermost TPS material that would interact with the convection. The results from the data analysis can be seen in Figure 36, Figure 37, and Figure 38.
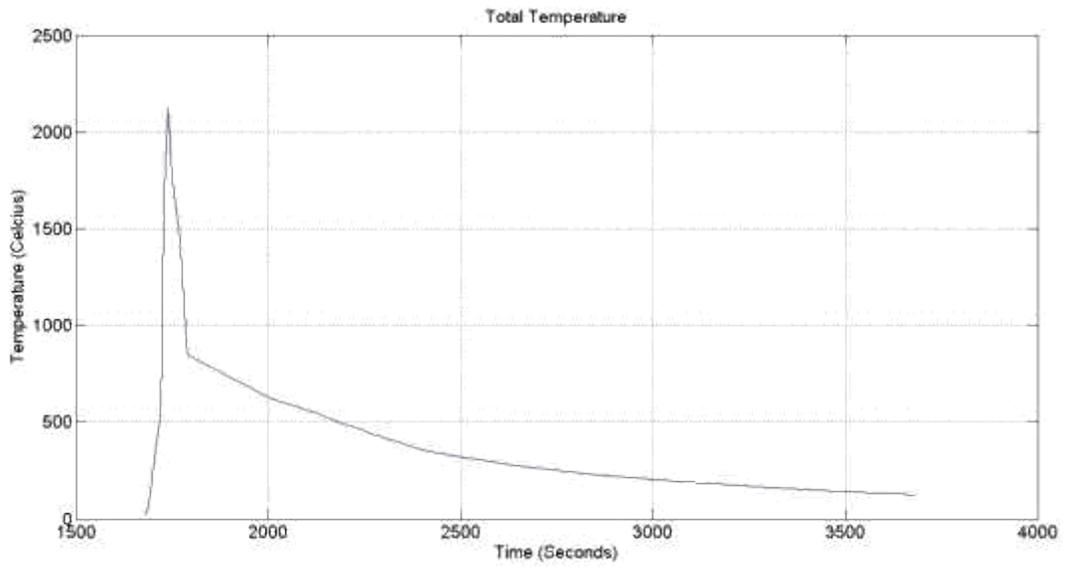
Figure 36: Total Descent Temperature

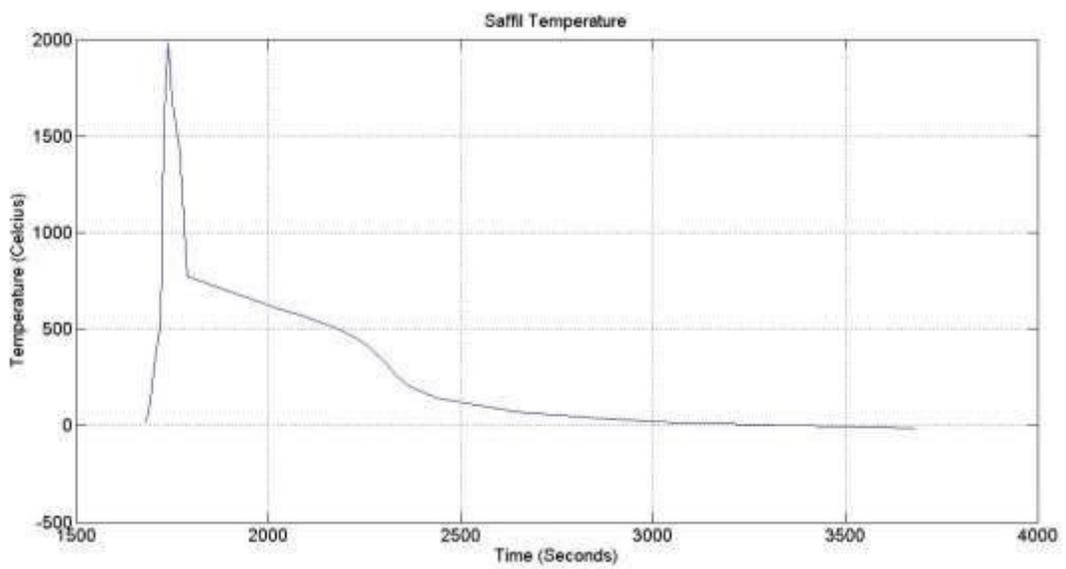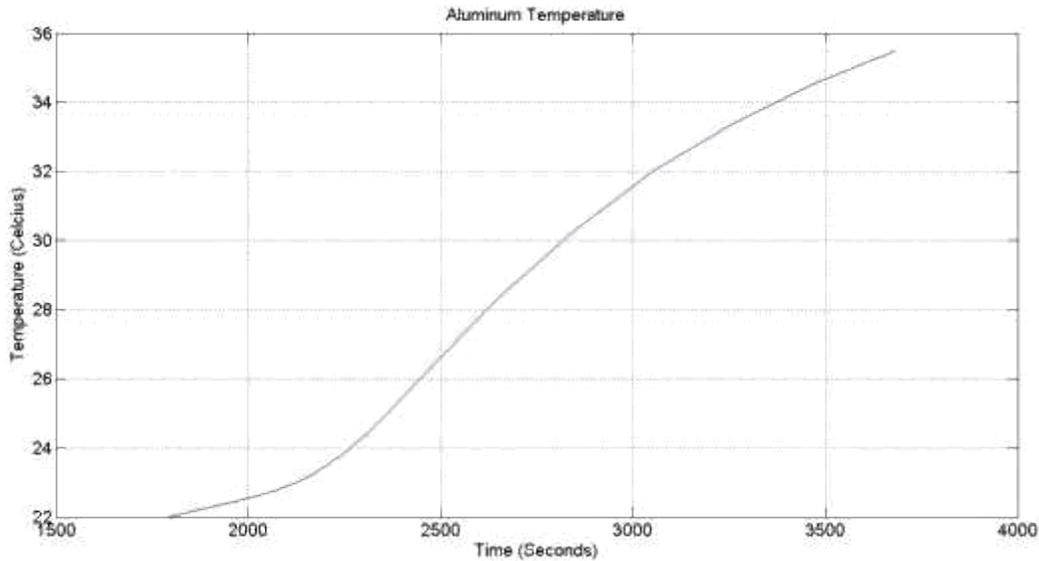**Figure 37: Saffil Descent Temperature**

37

Figure 38: Aluminum Descent Temperature

As seen in Figure 36 the maximum temperature occurs at around 1740 seconds at a value of 2400°C. This temperature coincides with the maximum convection that occurs during the descent trajectory. This temperature occurs on the RCC honeycomb layer which re-radiates some of the thermal energy back into the flow and the rest is carried through the RCC to the Saffil by means of conduction. The Saffil temperature can be seen in Figure 37. This shows that the temperature of the Saffil is just below 2000°C. This maximum temperature is close to the melting point of the material but due to how short the temperature is at that point no damage is expected to occur and can be reused. The main interest to prove the viability of this TPS system is the temperature at the top of the aluminum substructure. Seen in Figure 38 the maximum temperature the aluminum plate reaches is about 35°C. This is far better than what was expected when conducting the thermal analysis. Unfortunately the temperature seems to continue to rise for a longer period but it occurs after touchdown and is expected to be far less than the melting point of the aluminum structure.

9.4 Total Mass

The total dry mass and wet mass of the waverider was calculated. The Dry mass was used for the sizing of length of the waverider. The dry and wet masses can be seen in Table 11and Table 12.

Table 11: Total Dry Mass

Dry Mass Design Variable (lb)	Design
Thermal Mass	41391.1
Structural Mass	78091.46
Fuel Tank Mass	8013.11
Oxidizer Tank Mass	24.127.6
Engine Mass	2723
Payload Mass	2000
Total Dry Mass	132218.7

Table 12: Total Wet Mass

Wetted Mass Design Variable (lb)	Design
Thermal Mass	41391.1
Structural Mass	78091.46
Fuel Tank Mass	8013.11
Oxidizer Tank Mass	24.127.6
Engine Mass	2723
Payload Mass	2000
Fuel Mass	169038
Oxidizer Mass	437167
Total Wet Mass	738423.7

As seen in the previous tables the dry mass of the waverider is calculated to be 132218.7 lbs. This mass includes the TPS, Structures, Fuel and Oxidizer tanks, Engine mass, and Payload mass. The dry mass is significant because it directly determines how long the tanks and therefore the waverider needed to be in order to complete a mission. The wet mass includes the fuel and oxidizer mass for the propellants after being calculated. The total wet mass calculates out to be 738423.7 lbs.

10.0 CONCLUSION

This study of the hypersonic launch vehicle undertook various aspects of the design process of the vehicle. The first was the mission was outlined, second the preliminary design of the craft was defined, and third the detailed design, analysis and optimization of the vehicle were performed.

The vehicles aerodynamics, propulsion and thermal dynamics were closely analyzed for the optimal sizing of the waverider for a given trajectory. It was found that a waverider 135 ft. long would be sufficient to house the payload bay, fuel tank and oxidizer tank. The Aerodynamics had a maximum L/D of 4.5 for the trajectory and over 6 for Mach 18. This proves that the waverider had a minimum spillage of high pressure to the low pressure. The propulsion system calculated the total mass of fuel needed to be 169038 lbs. and a total mass of oxidizer to be 437167 lbs. The thermal protection system was analyzed using the convection data obtained from CBAERO and the analysis showed that at a maximum convection the temperature of the Saffil insulation would be less than 2000°C and the aluminum temperature would be around 35°C.

11.0 RECOMMENDATIONS

This is an initial study that would require a detailed structural concept to be developed. Also this study did not conduct analysis on the control of the waverider which is crucial to a fully designed model. This could change the aerothermal analysis if a v-tail is required for control authority. A full analysis of the trajectory is required. CBAERO is a great tool for initial design space but a higher order accuracy aerothermal code will be required for the detailed analysis of the trajectory for verification. The design of a specialized trajectory might be able to maximize the range for the craft and would be helpful instead of using a given trajectory.

BIBLIOGRAPHY

[1] S. Garber, "Sputnik and The Dawn of the Space Age," NASA, 10 October 2007. [Online]. Available: http://history.nasa.gov/sputnik/. [Accessed 8 September 2013].

[2] R. R. GILRUTH, "Apollo Expeditions to the Moon," NASA, 28 July 1975. [Online]. Available: http://history.nasa.gov/SP-350/ch-2-1.html. [Accessed 9 SEPTEMBER 2013].

[3] J. Heyman, " Directory of U.S. Military Rockets and Missiles," Designation-Systems.Net, 25 June 2009. [Online]. Available: http://www.designation-systems.net/dusrm/app3/index.html. [Accessed 8 September 2013].

[4] J. D. A. Jr., "Fundamentals of Aerodynamics," in *Fundamentals of Aerodynamics*, New York McGraw-Hill, 2007, p. 888.

[5] R. E. Graves, "Aerodynamic Performance of Osculating-Cones Waveriders at High Altitudes," Graduate School of the University of Colorado, Boulder, 1999.

[6] S. Staff, "Gallery: DARPA's Falcon Hypersonic Glider's Mach 20 Launch Test," Space.com, 10 August 2011. [Online]. Available: http://www.space.com/12604-darpa-hypersonic-glider-falcon-htv2-photos.html. [Accessed 9 September 2013].

[7] N. A. a. S. Museum, "Apollo 11 Command Module "Columbia"," [Online]. Available: http://airandspace.si.edu/events/apollo11/objects/apolloartifact.cfm?id=A19700102000. [Accessed 9 September 2013].

[8] NASA, Systems Engineering Handbook, NASA, 1995.

[9] D. K. Huzel and H. D. H, Modern Engineering for Design of Liquid-Propellant Rocket Engines, SW: American Institute of Aeronautics and Astronautics, 1992.

[10] AIAA, Aerospace Design Engineers Guide, Reston: American Institute of Aeronautics and Astronautics Inc., 2003.

[11] M. A. Lobbia, "A Framework for the Design and Optimization of Waverider-Derived Hypersonic Transport Configurations," University of Tokyo, Tokyo, 2004.

[12] H. J, F. J. S and W. R. E, "MODIFICATION AND VERIFICATION TESTING OF A RUSSIAN NK-33 ROCKET ENGINE FOR REUSABLE AND RESTARTABLE APPLICATIONS," in *34th AIAA/ASME/SAE/ASEE Joint Propulsion Conference*, Cleveland, 1998.

[13] J. Roskam, Airplane Design Part III, Lawrence: DAR Corporation, 2002.

[14] D. J. Kinney, "Aero-Thermodynamics for Conceptual Design," NASA Ames Research Center, Mountain View, 2004.

[15] M. L. Blosser, "Development of Metallic Thermal Protection Systems for the Reusable Launch Vehicle," National Aeronautics and Space Administration, Hampton, 1996.

[16] Matweb, "Aluminum 2024-T81," Matweb, 2014. [Online]. Available: http://www.matweb.com/search/datasheet.aspx?matguid=6441f805a3bb42758ab5b15752343138&ckck=1. [Accessed 21 March 2014].

[17] P. Blau, "Antares Launch Vehicle Information," Spaceflight101, 2013. [Online]. Available: http://www.spaceflight101.com/antares-launch-vehicle-information.html. [Accessed 1 December 2013].

[18] O. S. CORPORATION, "Taurus II Users Manual," 2009.

APPENDIX

Material	Temperature	Value	Units
Al 2024-T81			
Density		2780	kg/m^3
Thermal Conductivity	-100	114	W/mC
	0	144	W/mC
	100	165	W/mC
	200	175	W/mC
Specific Heat		875	J/kgC
RCC Honeycomb Sandwich			
Density		270	kg/m^3
Thermal Conductivity		35	W/mC
Specific Heat		710	J/kgC
Saffil			
Density		48	kg/m^3
Thermal Conductivity	20	0.01	W/mC
	150	0.015	W/mC
	220	0.02	W/mC
	300	0.025	W/mC
	380	0.03	W/mC
	450	0.04	W/mC
	500	0.05	W/mC
	700	0.12	W/mC
	2700	0.12	W/mC
Specific Heat		1000	J/kgC